

## $\beta$ -D-Xylosidase From *Selenomonas ruminantium* of Glycoside Hydrolase Family 43

DOUGLAS B. JORDAN,<sup>\*,1</sup> XIN-LIANG LI,<sup>1</sup>  
CHRISTOPHER A. DUNLAP,<sup>2</sup> TERENCE R. WHITEHEAD,<sup>1</sup>  
AND MICHAEL A. COTTA<sup>1</sup>

<sup>1</sup>Fermentation Biotechnology Research Unit, National Center  
For Agricultural Utilization Research, US Department of Agriculture,  
Agricultural Research Service, <sup>†</sup>1815 N. University Street, Peoria, IL 61604,  
E-mail: jordand@ncaur.usda.gov; and <sup>2</sup>Crop Bioprotection Research Unit,  
National Center For Agricultural Utilization Research, US Department of  
Agriculture, Agricultural Research Service, 1815 N. University Street,  
Peoria, IL 61604

### Abstract

$\beta$ -D-Xylosidase from the ruminal anaerobic bacterium, *Selenomonas ruminantium* (SXA), catalyzes hydrolysis of  $\beta$ -1,4-xylooligosaccharides and has potential utility in saccharification processes. The enzyme, heterologously produced in *Escherichia coli* and purified to homogeneity, has an isoelectric point of approx 4.4, an intact N terminus, and a Stokes radius that defines a homotetramer. SXA denatures between pH 4.0 and 4.3 at 25°C and between 50 and 60°C at pH 5.3. Following heat or acid treatment, partially inactivated SXA exhibits lower  $k_{\text{cat}}$  values, but similar  $K_{\text{m}}$  values as untreated SXA. D-Glucose and D-xylose protect SXA from inactivation at high temperature and low pH.

**Index Entries:** Fuel ethanol; glycohydrolase; hemicellulose; protein stability; saccharification; arabinofuranosidase; inhibitors; catalysis.

### Introduction

$\beta$ -D-Xylosidase (EC 3.2.1.37) catalyzes hydrolysis of  $\beta$ -1,4 glycosidic bonds linking D-xylose residues that form xylooligosaccharides (1–7). In conjunction with  $\beta$ -xylanases, which cleave larger polymers of D-xylose (xylans) to xylooligosaccharides,  $\beta$ -xylosidase serves to depolymerize xylan, a major component of plant cell walls and one of the most abundant biopolymers in nature. Auxiliary enzymes catalyze hydrolysis of sugar

\*Author to whom all correspondence and reprint requests should be addressed.

<sup>†</sup>The mention of firm names or trade products does not imply that they are endorsed or recommended by the US Department of Agriculture over other firms or similar products not mentioned.

and acid side chains from the xylose residues. A goal of this laboratory and others is to identify catalytically efficient and robust enzymes that promote complete saccharification of xylans to monosaccharides for fermentation to fuel ethanol and other bioproducts.

Previous studies have shown that strains of the ruminal anaerobic bacterium, *Selenomonas ruminantium*, can enhance utilization of xylooligosaccharides under fermentation conditions (8–10). A crude preparation of  $\beta$ -xylosidase from *S. ruminantium* GA192 (SXA), cloned and expressed in *Escherichia coli*, was shown to catalyze hydrolysis of 4-nitrophenyl- $\beta$ -D-xylopyranoside (4NPX) and 4-nitrophenyl- $\alpha$ -L-arabinofuranoside with 10-fold preference for the former substrate over the latter (11). Appositely, the preparation of SXA can catalyze hydrolysis of oligosaccharides, produced from partial hydrolysis of oat spelt xylan and wheat arabinoxylan, to smaller oligosaccharides, D-xylose and L-arabinose (11).

The amino acid sequence of SXA places it within glycoside hydrolase family 43. Recently, X-ray structures of glycoside hydrolase family 43  $\beta$ -xylosidases have been deposited in the Protein Data Bank (<http://www.pdb.org/>) for the enzyme from *Clostridium acetobutylicum*, *Bacillus subtilis*, and *B. halodurans*. The X-ray structures describe homotetrameric proteins with monomers consisting of two domains, one of which is similar to the five-bladed  $\beta$  propeller domain found in a GH family 43 arabinanase from *Cellvibrio cellulosa* (12), which is a homodimer of monomers of the single domain. Protein sequence identity of SXA against the family 43  $\beta$ -xylosidases with reported X-ray structures is 53–72%, making the X-ray structures useful in generating three-dimensional models of SXA. In this work, we explore practical properties of SXA with respect to saccharification of hemicellulose. Destabilization of SXA by extremes of pH and temperature, counteracting stabilization of SXA by monosaccharides, and the pH dependence of monosaccharide binding (inhibition of SXA catalysis) are reported.

## Materials and Methods

### Materials and General Methods

The gene encoding  $\beta$ -xylosidase from *S. ruminantium* GA192 was cloned and expressed in *E. coli* as described (11). SXA, produced in *E. coli*, was purified to homogeneity, as judged from SDS-PAGE analysis, by using reverse phase and anionic exchange chromatography steps. Concentrations of homogeneous SXA monomers (active sites) were determined by using an extinction coefficient at 280 nm of 129,600/M/cm, calculated from amino acid composition (13). N-terminal Edman sequencing was conducted by the Wistar Proteomics Facility (Philadelphia, PA). Buffers and 4NPX were obtained from Sigma-Aldrich (St. Louis, MO). All other reagents were reagent grade and high purity. A Cary 50 Bio UV-Visible spectrophotometer (Varian; Palo Alto, CA), equipped with a thermostatted holder for cuvettes, was used for spectral and kinetic determinations. Delta extinction coefficients

(product–substrate) at 400 nm were determined for each buffer condition by subtracting the molar absorbance of 4NPX from that of 4-nitrophenol (4NP). The concentration of 4NP was determined by using the published extinction coefficient of 18.3/mM/cm at 400 nm for 4NP in NaOH (14). The concentration of 4NPX was determined by incubating the substrate with excess enzyme until an end point was reached, adding an aliquot (0.01–0.1 mL) to 0.1 M NaOH, recording the absorbance at 400 nm and using the extinction coefficient of 18.3/mM/cm for 4NP. Data were fitted to linear and nonlinear equations by using the computer program Grafit (Erithacus Software; Surrey, UK). Manipulations of X-ray structure coordinates (overlays, distance measurements, and so on.) were through Swiss-PDB Viewer 3.7 (<http://www.expasy.org/spdbv/>) (15). The Stokes radius was calculated from X-ray coordinates of the homologous  $\beta$ -xylosidase from *C. acetobutylicum* (PDB ID: 1YI7) by using the computer program HYDROPRO, Version 7.C (16). HYDROPRO (Freeware available at <http://leonardo.rev.vm.es/macromol/programs/hydropro/hydropro.html>) computes hydrodynamic properties of rigid macromolecules from their atomic-level structure.

#### *Molecular Mass, Quaternary Structure, and Isoelectric Point SXA*

SDS-PAGE analysis was conducted by using a Criterion gel system, Criterion Tris-HCl 8–16% polyacrylamide gels, Bio-Safe stain, and protein molecular weight standards (all from Bio-Rad Laboratories; Hercules, CA). The Stokes radius of SXA was determined by using a gel filtration method: the column ( $2.6 \times 62 \text{ cm}^2$ ) was packed with Toyapearl 55F resin (Tosoh Bioscience; Montgomeryville, PA) and equilibrated with 100 mM sodium phosphate, pH 7.0 at 24–26°C (room temperature) with a flow rate of 2.0 mL/min. Postcolumn eluate was monitored continuously for absorbance at 260, 280, and 405 nm. Elution volumes ( $V_e$ ) were recorded and transformed to  $K_{av}$  values by using Eq. 1, where  $V_e$  is the recorded elution volume,  $V_0$  is the void volume of the column, and  $V_t$  is the total volume of the column plus tubing to the absorbance monitor. The value for  $V_0$  was determined as 112 mL by using blue dextran 2000. The value of  $V_t$  was determined as 330 mL. Protein standards of known Stokes radius ( $R_s$ ) and molecular weight (MW) were obtained from GE Healthcare Life Sciences (Piscataway, NJ): ferritin ( $R_s = 61.0 \text{ \AA}$  and MW = 440 kDa), catalase ( $R_s = 52.2 \text{ \AA}$  and MW = 232 kDa), and aldolase ( $R_s = 48.1 \text{ \AA}$  and MW = 158 kDa). The Stokes radius of SXA was determined from the linear regression of protein standards fitted to eq. 2 where  $K_{av}$  is the transformed value of  $V_e$ ,  $R_s$  is the Stokes radius,  $m$  is the slope and  $C$  is the constant of the standard line.

$$K_{av} = \frac{V_e - V_0}{V_t - V_0} \quad (1)$$

$$(\text{Log}K_{av})^{1/2} = m \times R_s + C \quad (2)$$

Isoelectric focusing (IEF) was conducted by using a Criterion electrophoresis system, Criterion pH 3.0–10.0 gels, IEF standards, and Coomassie R-250/Crocein Scarlet IEF gel stain (all from Bio-Rad; Hercules, CA).

#### *pH Stability of SXA at 25°C*

Buffers of constant ionic strength ( $I = 0.3\text{ M}$ ), adjusted with NaCl, were used as indicated: 100 mM succinate–NaOH (pH 3.5–6.0), 100 mM sodium phosphate (pH 6.0–8.0), 30 mM sodium pyrophosphate (pH 8.0–9.0), and 100 mM glycine–NaOH (pH 9.0–10.0). For preincubation, an aliquot (7  $\mu\text{L}$ ) of SXA (168  $\mu\text{M}$  with respect to monomer concentration in 50 mM Tris-HCl, pH 7.5) was added to 100  $\mu\text{L}$  of buffered solutions at varied pH and 25°C. For ligand protection studies, varied concentrations of D-xylose or D-glucose were included in or omitted from the 100- $\mu\text{L}$  preincubation mixtures containing 100 mM succinate–NaOH, pH 4.0, adjusted with NaCl to  $I = 0.3\text{ M}$ . At varied times after enzyme addition, 7  $\mu\text{L}$  of preincubation mixtures were added to 1-mL reaction mixtures containing 100 mM sodium phosphate, pH 7.0, adjusted with NaCl to  $I = 0.3\text{ M}$  (buffer A), and 1.95 mM 4NPX at 25°C. Initial rates were determined by monitoring reactions continuously at 400 nM for 0.3 min. For determination of the expression, “relative activity remaining”, initial rates were divided by the rate of enzyme preincubated in buffer A at 0°C and assayed in 1-mL reaction mixtures containing the concentration of monosaccharide (corresponding to the carryover from enzyme preincubated in monosaccharide), the concentration of preincubation buffer (corresponding to the carryover from preincubated enzyme), and 1.95 mM 4NPX in buffer A at 25°C. Relative activity remaining data were fitted to Eq. 3, which describes a first-order decay:  $A$  is the relative activity remaining at varied times of preincubation,  $A_0$  is the relative activity remaining at time zero of the preincubation,  $k_{\text{obs}}$  is the first-order rate constant, and  $t$  is the time of preincubation. Apparent affinities for D-xylose and D-glucose were determined by fitting  $k_{\text{obs}}$  values from the monosaccharide protection studies to Eq. 4 where  $k_{\text{obs}}$  is the observed first-order rate constant for the decay,  $k_0$  is the first-order rate constant in the absence of ligand (e.g., D-xylose),  $I$  is the ligand concentration in the preincubation mixture, and  $K_i$  is the dissociation constant of ligand from the enzyme-ligand complex.

$$A = A_0 \times e^{-k_{\text{obs}} \times t} \quad (3)$$

$$k_{\text{obs}} = \frac{k_0}{1 + I/K_i} \quad (4)$$

To determine the effect on steady-state kinetic parameters caused by low pH treatment, SXA was preincubated in 100 mM succinate–NaOH, pH 4.0 (adjusted with NaCl to  $I = 0.3\text{ M}$ ) at 25°C until approx 50% of

its catalytic activity was degraded (assessed from reactions containing 1.95 mM 4NPX in buffer A at 25°C), the pH of the preincubation mixture was raised to pH 4.9 (where SXA is stable) by adding an equal volume of buffer A at 0°C and mixing 7  $\mu$ L of the pH-adjusted mixture were added to 1-mL reactions containing varied concentrations of 4NPX (0.2–5.0 mM) in buffer A at 25°C, and the reactions were monitored continuously at 400 nm for 0.3 min to determine initial rates. Initial rates of catalysis were fitted to Eq. 5 where  $v$  is the initial rate at a specified concentration of 4NPX,  $k_{\text{cat}}$  is the rate of catalysis when enzyme is saturated with substrate,  $S$  is the substrate concentration, and  $K_m$  is the Michaelis constant. The parameter,  $k_{\text{cat}}$ , is expressed in moles of substrate hydrolyzed per second per mole of enzyme active sites (monomers), calculated using the delta extinction coefficient for 4NP–4NPX at 400 nm and the extinction coefficient for SXA at 280 nm.

$$v = \frac{k_{\text{cat}} \times S}{K_m + S} \quad (5)$$

### Thermal Stability of SXA at pH 5.3

For preincubation, 7  $\mu$ L of SXA (168  $\mu$ M with respect to monomer concentration in 50 mM Tris-HCl, pH 7.5) were added to 100  $\mu$ L of 100 mM succinate–NaOH, pH 5.3 (adjusted with NaCl to  $I = 0.3$  M) at varied temperatures. Ligand protection studies contained varied concentrations of D-xylose or D-glucose in the pH 5.3 preincubation buffer at 55°C. At varied times after enzyme addition, 15  $\mu$ L of the preincubation mixtures were added to 15  $\mu$ L of buffer A at 0°C to cool and bring the pH to 6.3, 7  $\mu$ L of the enzyme mixture at 0°C were added to 1-mL reaction mixtures containing 1.95 mM 4NPX in buffer A at 25°C, and initial rates were determined by monitoring reactions continuously at 400 nm for 0.3 min. The expression, “relative activity remaining”  $k_{\text{obs}}$ , and  $K_i$  were determined from the initial rate data as described in the Section pH Stability of SXA at 25°C.

To determine the effect on steady-state kinetic parameters caused by heat treatment, SXA was preincubated in 100 mM succinate–NaOH, pH 5.3 ( $I = 0.3$  M) at 55°C until approx 50% of its catalytic activity was degraded (assessed from reactions containing 1.95 mM 4NPX in buffer A at 25°C), the temperature of the preincubation mixture was lowered by adding an equal volume of buffer A at 0°C, 7  $\mu$ L of the cooled enzyme mixture were added to 1-mL reactions containing varied concentrations of 4NPX (0.2–5.0 mM) in buffer A at 25°C, and the reactions were monitored continuously at 400 nm for 0.3 min to determine initial rates of catalysis. Steady-state kinetic parameters were determined by fitting initial-rate data to Eq. 5 as described in the Section pH Stability of SXA at 25°C.

### Inhibition of SXA-Catalyzed Hydrolysis of 4NPX by D-Glucose and D-Xylose

The 1-mL reaction mixtures at 25°C contained varied concentrations of 4NPX and varied concentrations of D-glucose or D-xylose in buffers of constant ionic strength ( $I = 0.3\text{ M}$ , adjusted with NaCl) as indicated in the Section pH Stability of SXA at 25°C. Reactions were initiated by addition of 7  $\mu\text{L}$  of SXA, preincubated in 10 mM sodium phosphate, pH 7.0 at 0°C. Reactions were monitored continuously for 0.3 min at 400 nm to determine initial rates. Initial-rate data were fitted to Eq. 6, where  $v$  is the initial rate,  $k_{\text{cat}}$  is the rate of the reaction when saturated with substrate,  $S$  is the substrate concentration,  $K_{\text{m}}$  is the Michaelis constant,  $I$  is the inhibitor concentration (e.g., D-glucose), and  $K_{\text{i}}$  is the dissociation constant of inhibitor from the enzyme-inhibitor complex.

$$v = \frac{k_{\text{cat}} \times S}{K_{\text{m}} (1 + I/K_{\text{i}}) + S} \quad (6)$$

## Results and Discussion

The gene encoding for SXA predicts a protein of 538 amino acids and a molecular mass of 61,140 Da. Edman sequencing of the first ten residues starting at the N terminus of SXA indicated the sequence, MNIQNPVLKG, which agrees with the sequence predicted from the gene and indicates that SXA is produced by *E. coli* with an intact N terminus. SDS-PAGE analysis shows that the purified SXA is homogeneous with a molecular mass of approx 60 kDa (Fig. 1A).

We chose the structure of  $\beta$ -xylosidase from *C. acetobutylicum* (PDB ID: 1YI7) for modeling of SXA because of its 72% protein sequence identity to SXA; as well, within a 9 Å sphere of the active site of 1YI7, all 21 residues are identical in the sequence of SXA. The X-ray coordinates of  $\beta$ -xylosidase from *C. acetobutylicum* contain 534 amino acid residues per subunit of the homotetramer, four fewer residues per subunit than the sequence of SXA. The longest axis of the homotetramer of  $\beta$ -xylosidase from *C. acetobutylicum* is calculated as 123 Å by using the computer program HYDROPRO, and the longest distance, perpendicular to this axis, is approx 90 Å as measured from the coordinates of the tetramer. We determined the Stokes radius of SXA by using a gel filtration method (Fig. 1B). The determined value of  $55.4 \pm 0.5$  Å for the Stokes radius of SXA is similar to the value of 52 Å, calculated by using HYDROPRO and the X-ray structure coordinates of homotetrameric  $\beta$ -xylosidase from *C. acetobutylicum*; consistent with SXA occurring as a homotetramer in solution.

The isoelectric point of native SXA (estimated as approx 4.4) is slightly lower than the lowest isoelectric point (4.5) of the protein standards, but clearly well above the lowest pH (pH = 3.0) of the gel (Fig. 2A).

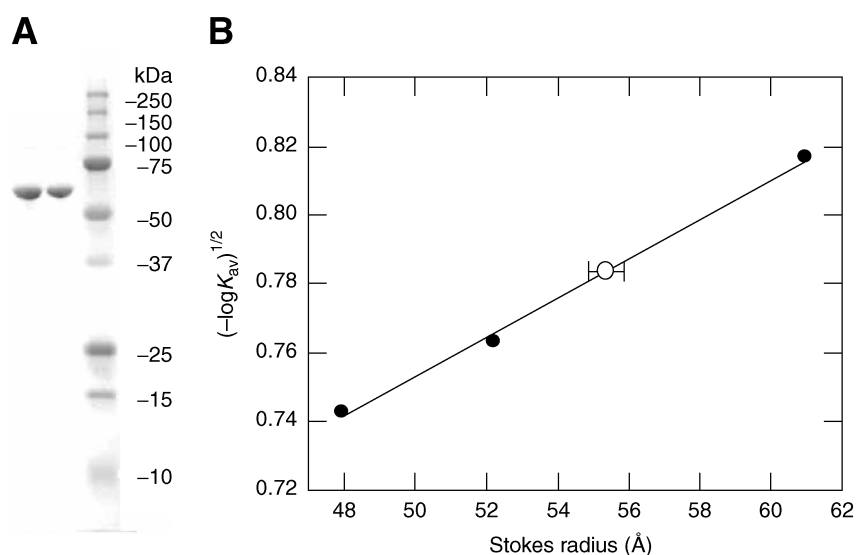


**Fig. 1.** Molecular mass and size of heterologously-produced SXA. **(A)** SDS-PAGE analysis of SXA. From left to right are lanes containing 1 µg SXA, 0.5 µg SXA, protein standards, and molecular masses (in kDa) of the protein standards. **(B)** Stokes radius of SXA.  $K_{av}$  values were determined for protein standards (●) of known Stokes radius and the line was drawn by fitting the values to Eq. 2. SXA (○) is positioned by using the value determined for  $K_{av}$  and the value determined for its Stokes radius (RS) ± the standard error of the estimate of the standard line (RS = 55.4 ± 0.5 Å).

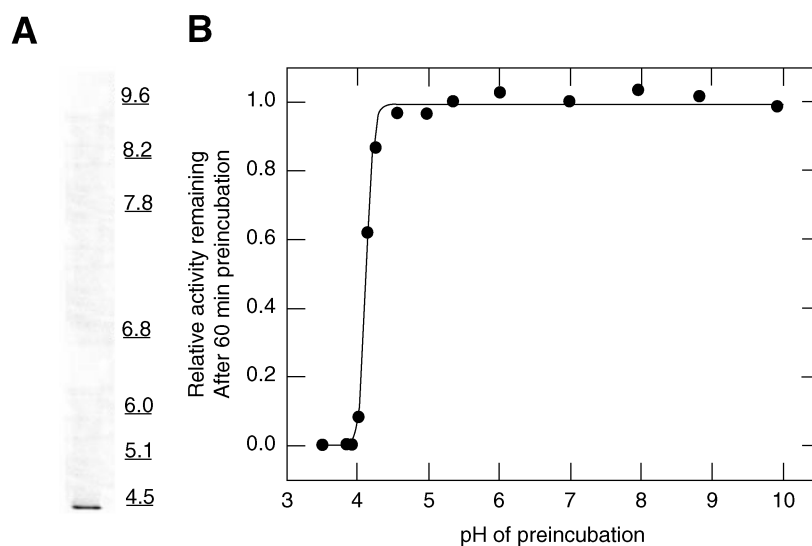


**Fig. 2.** Influence of pH on SXA. **(A)** IEF of native SXA. The left lane contains 0.5 µg SXA. The right lane indicates the positions of protein standards of known isoelectric point. **(B)** pH stability of SXA catalytic activity. SXA was preincubated at the indicated pH values and 25°C for 60 min before analyzing for relative activity remaining (catalytic activity relative to SXA preincubated at 0°C and pH 7.0). Standards deviations (±) of at least three determinations are indicated. The curve is drawn as a visual aid.

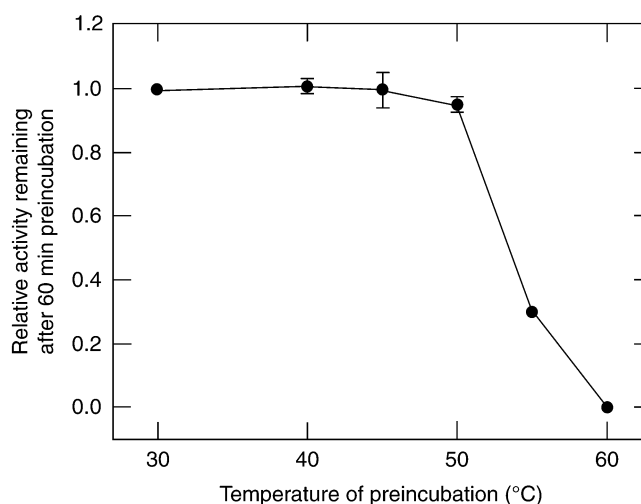


**Fig. 3.** Influence of temperature on SXA stability. SXA was preincubated at the indicated temperatures and pH 5.3 for 60 min before analyzing for relative activity remaining (catalytic activity relative to SXA preincubated at 0°C and pH 7.0). Standards deviations ( $\pm$ ) of at least three determinations are indicated. The curve is drawn as a visual aid.

SXA is inactivated by conditions of low pH and high temperature, with a sharp drop in activity between pH 4.0 and 4.3 at 25°C (Fig. 2B) and a broad drop between 50 and 60°C at pH 5.3 (Fig. 3). Loss of catalytic activity at low pH and high temperature was associated with cloudiness in the preincubation mixtures, suggesting that SXA denatures and precipitates. To determine the effect of partially inactivated SXA on steady-state kinetic parameters, the enzyme was preincubated at pH 4.0 and 25°C or at pH 5.3 and 55°C until approx 50% of its catalytic activity remained in each sample. The preincubated samples of SXA were pH adjusted and cooled before the determination of kinetic parameters by fitting initial-rate data (obtained at pH 7.0 and 25°C) to Eq. 5 for comparison with an untreated SXA control sample: partially pH-inactivated SXA ( $k_{\text{cat}} = 6.36 \pm 0.041 \text{ s}^{-1}$  and  $K_{\text{m}} = 0.366 \pm 0.014 \text{ mM}$ ); partially temperature-inactivated SXA ( $k_{\text{cat}} = 5.39 \pm 0.062 \text{ s}^{-1}$  and  $K_{\text{m}} = 0.386 \pm 0.084 \text{ mM}$ ); and untreated control SXA ( $k_{\text{cat}} = 12.2 \pm 0.05 \text{ s}^{-1}$  and  $K_{\text{m}} = 0.380 \pm 0.005 \text{ mM}$ ). Thus, inactivation by low pH or high temperature is attributed to degradation of the  $k_{\text{cat}}$  parameter without changing  $K_{\text{m}}$ , consistent with the view that, on limited exposure to the extreme conditions, a portion of the protein denatures and does not contribute to the catalyzed hydrolysis of 4NPX. Complementary experiments have shown that inactivation of SXA by low pH or high temperature is not reversible by simply adjusting the pH or cooling.

At pH 5.3 and 55°C, SXA is inactivated in a first-order process with a rate constant of  $0.0252 \pm 0.0020 \text{ min}^{-1}$  (Fig. 4A). SXA was protected from

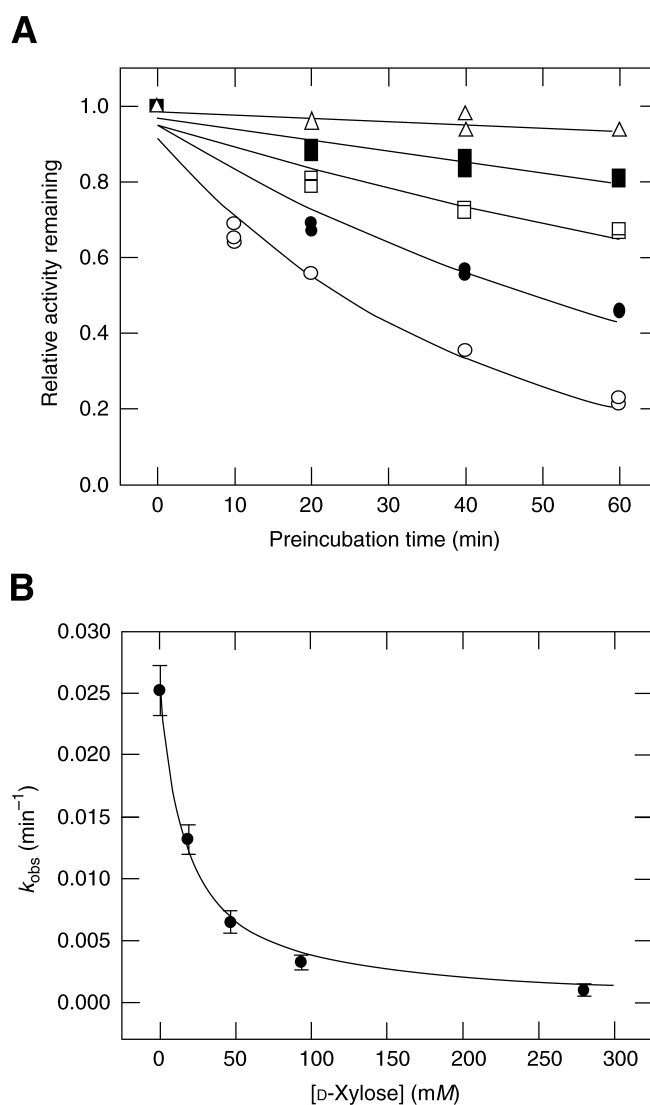


**Fig. 4.** Protection of SXA from thermal inactivation at 55°C by D-xylose. **(A)** Decay curves. Before analyzing for relative activity remaining, SXA was preincubated for the indicated times at pH 5.3 and 55°C in the absence (○) or presence of D-xylose at 18.7 mM (●), 46.7 mM (□), 93.5 mM (■), and 280 mM (△). Progress curves were generated by fitting the data for each D-xylose concentration to Eq. 3: 0 mM ( $k_{obs} = 0.0252 \pm 0.0020 \text{ min}^{-1}$ ), 18.7 mM ( $k_{obs} = 0.0132 \pm 0.0010 \text{ min}^{-1}$ ), 46.7 mM ( $k_{obs} = 0.00649 \pm 0.00087 \text{ min}^{-1}$ ), 93.5 mM ( $k_{obs} = 0.00326 \pm 0.00056 \text{ min}^{-1}$ ), and 280 mM ( $k_{obs} = 0.000917 \pm 0.00033 \text{ min}^{-1}$ ). **(B)** Dependence of first-order decay rates on the concentration of D-xylose. The  $k_{obs}$  values determined from the decay rates of panel A ( $\pm$  standard errors) are plotted vs the D-xylose concentration of each preincubation condition. The curve was generated by fitting the  $k_{obs}$  values to Eq. 4:  $K_{i(\text{D-xylose})} = 17.6 \pm 1.8 \text{ mM}$ .

thermal denaturation by including in the preincubation mixture varied concentrations of D-xylose. Protection from temperature denaturation was dependent on the concentration of D-xylose (Fig. 4A), and as the concentration of D-xylose approached saturation the decay rate approaches zero (Fig. 4B), in accordance with Eq. 4, which estimates a dissociation constant ( $K_i = 17.6 \pm 1.8 \text{ mM}$ ) for D-xylose from the  $k_{\text{obs}}$  values (Fig. 4B). This 55°C value compares with a 25°C value ( $K_i = 7.62 \pm 0.26 \text{ mM}$ ) for inhibition of SXA-catalyzed hydrolysis of 4NPX at pH 5.3 and 25°C by D-xylose. Similarly, SXA was protected from thermal denaturation (55°C at pH 5.3) by including in the preincubation mixture varied concentrations of D-glucose; denaturation rates, determined by fitting the decay data for each D-glucose concentration to Eq. 3, were 0 mM ( $k_{\text{obs}} = 0.0256 \pm 0.0015 \text{ min}^{-1}$ ), 93.5 mM ( $k_{\text{obs}} = 0.00949 \pm 0.00069 \text{ min}^{-1}$ ), 187 mM ( $k_{\text{obs}} = 0.00588 \pm 0.00077 \text{ min}^{-1}$ ), 280 mM ( $k_{\text{obs}} = 0.00445 \pm 0.00081 \text{ min}^{-1}$ ), and 374 mM ( $k_{\text{obs}} = 0.00336 \pm 0.00095 \text{ min}^{-1}$ ). A dissociation constant ( $K_i = 56.1 \pm 0.8 \text{ mM}$ ) was estimated for D-glucose from fitting the  $k_{\text{obs}}$  values to Eq. 4. This 55°C value compares with a 25°C value ( $K_i = 79.0 \pm 2.3 \text{ mM}$ ) for inhibition of SXA-catalyzed hydrolysis of 4NPX at pH 5.3 and 25°C by D-glucose.

At pH 4.0 and 25°C, SXA is inactivated in a first-order process with a rate constant of  $0.0784 \pm 0.0023 \text{ min}^{-1}$ , and protection from denaturation at low pH is dependent on the concentration of D-xylose (Fig. 5A). Protection from pH denaturation by D-xylose is saturable with a first-order decay rate of zero at saturating D-xylose in accordance with Eq. 4, which estimates a dissociation constant ( $K_i = 31.7 \pm 2.8 \text{ mM}$ ) for D-xylose (Fig. 5B). This pH 4.0 value compares with a pH 4.3 value ( $K_i = 43.5 \pm 1.1 \text{ mM}$ ) for inhibition of SXA-catalyzed hydrolysis of 4NPX at pH 4.3 and 25°C by D-xylose. Similarly, inactivation rates of SXA at pH 4.0 and 25°C are slowed by D-glucose; denaturation rates, determined by fitting the decay data for each D-glucose concentration to Eq. 3, were 0 mM ( $k_{\text{obs}} = 0.0518 \pm 0.0037 \text{ min}^{-1}$ ), 234 mM ( $k_{\text{obs}} = 0.0210 \pm 0.0016 \text{ min}^{-1}$ ), 467 mM ( $k_{\text{obs}} = 0.0124 \pm 0.0007 \text{ min}^{-1}$ ), and 701 mM ( $k_{\text{obs}} = 0.00748 \pm 0.00083 \text{ min}^{-1}$ ). A dissociation constant ( $K_i = 147 \pm 12 \text{ mM}$ ) was estimated for D-glucose from fitting the  $k_{\text{obs}}$  values to Eq. 4. This pH 4.0 value compares with a pH 4.3 value ( $K_i = 330 \pm 8 \text{ mM}$ ) for inhibition of SXA-catalyzed hydrolysis of 4NPX at pH 4.3 and 25°C by D-glucose.

The influence of pH on inhibition of SXA-catalyzed hydrolysis of 4NPX by D-glucose and D-xylose was determined at 25°C by using buffers of constant ionic strength ( $I = 0.3 \text{ M}$ ). D-Glucose and D-xylose inhibited the catalyzed reaction competitively with respect to substrate 4NPX at all pH values examined in accordance with Eq. 6.  $K_i$  values for glucose decrease with increasing pH as follows: pH 4.3 ( $330 \pm 8 \text{ mM}$ ), pH 5.3 ( $79.0 \pm 2.3 \text{ mM}$ ), pH 7.0 ( $34.5 \pm 0.7 \text{ mM}$ ), and pH 9.0 ( $18.7 \pm 0.6 \text{ mM}$ ). Similarly, affinities of SXA for D-xylose increase with increasing pH as seen in the progression of  $K_i$  values: pH 4.3 ( $43.5 \pm 1.1 \text{ mM}$ ), pH 5.3 ( $7.62 \pm 0.26 \text{ mM}$ ), pH 7.0 ( $3.82 \pm 0.06 \text{ mM}$ ), and pH 9.0 ( $3.21 \pm 0.14 \text{ mM}$ ).

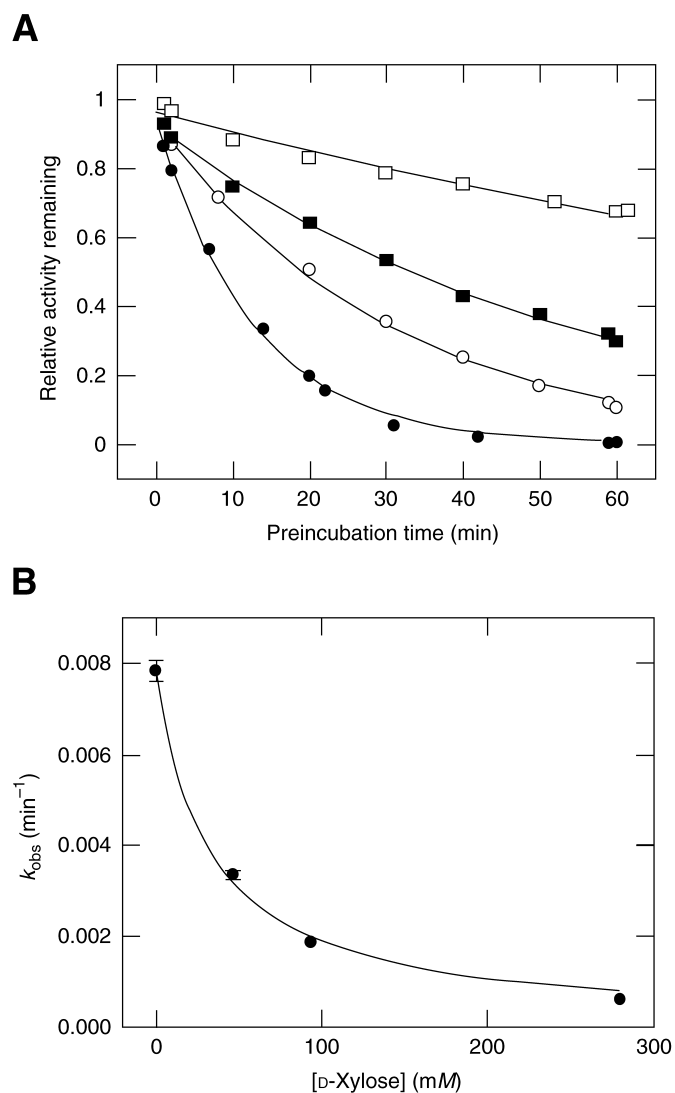


**Fig. 5.** Protection of SXA from low pH inactivation at pH 4.0 by D-xylose. **(A)** Decay curves. Before analyzing for relative activity remaining, SXA was preincubated for the indicated times at pH 4.0 and 25°C in the absence (●) or presence of D-xylose at 46.7 mM (○), 93.5 mM (■), and 280 mM (□). Progress curves were generated by fitting the data for each D-xylose concentration to Eq. 3: 0 mM ( $k_{obs} = 0.0784 \pm 0.0023 \text{ min}^{-1}$ ), 46.7 mM ( $k_{obs} = 0.0335 \pm 0.0008 \text{ min}^{-1}$ ), 93.5 mM ( $k_{obs} = 0.0186 \pm 0.0004 \text{ min}^{-1}$ ), and 280 mM ( $k_{obs} = 0.00614 \pm 0.00036 \text{ min}^{-1}$ ). **(B)** Dependence of first-order decay rates on the concentration of D-xylose. The  $k_{obs}$  values determined from the decay rates of panel A ( $\pm$  standard errors) are plotted vs the D-xylose concentration of each preincubation condition. The curve was generated by fitting the  $k_{obs}$  values to Eq. 4:  $K_{i(\text{D-xylose})} = 31.7 \pm 2.8 \text{ mM}$ .

Temperature and pH profiles of SXA stability place certain constraints on its application to processes for saccharification of the hemicellulose component of herbaceous biomass, as do  $K_i$  values for D-glucose and

D-xylose inhibition of SXA catalysis. Potentially, if saccharification processes require higher temperatures or lower pH than the native SXA withstands, SXA could be modified to better accommodate such assaults on its stability. Similarly, inhibition of catalysis by D-glucose and D-xylose, which constitute two major constituents of herbaceous biomass, potentially could be alleviated by protein engineering approaches. Three-dimensional models of SXA could aid in the design of such modifications. Native SXA is an efficient catalyst for the hydrolysis of xylooligosaccharides, details of which will be reported soon. Owing to the nature of SXA, negative influences of temperature and pH on protein stability and negative influences of inhibition of catalysis by D-glucose and D-xylose are not additive. That is, under conditions of low pH and/or high temperature, the presence of D-glucose and D-xylose could serve to stabilize SXA to an extent similar to their inhibition of catalysis. It is likely that oligosaccharide substrates of SXA afford similar protection from inactivation by low pH and high temperature.

## Acknowledgments

We thank Jay D. Braker and Patrick Kane for excellent technical assistance in contributing to this work.

## References

1. Zechel, D. L. and Withers, S. G. (2001), *Curr. Opin. Chem. Biol.* **5**, 643–649.
2. Vocadlo, D. J., Wicki, J., Rupitz, K., and Withers, S. G. (2002), *Biochemistry* **41**, 9727–9735.
3. Sinnott, M. L. (1990), *Chem. Rev.* **90**, 1171–1202.
4. Shallom, D., Leon, M., Bravman, T., et al. (2005), *Biochemistry* **44**, 387–397.
5. Saha, B. C. (2003), *J. Ind. Microbiol. Biotechnol.* **30**, 279–291.
6. Marshall, P. J. and Sinnott, M. L. (1983), *Biochem. J.* **215**, 67–74.
7. Herrmann, M. C., Vrsanska, M., Jurickova, M., Hirsch, J., Biely, P., and Kubicek, C. P. (1997), *Biochem. J.* **321**, 375–381.
8. Cotta, M. A. (1993), *Appl. Environ. Microbiol.* **59**, 3557–3563.
9. Williams, A. G., Withers, S. E., and Joblin, K. N. (1991), *Lett. Appl. Microbiol.* **12**, 232–235.
10. Cotta, M. A. and Whitehead, T. R. (1998), *Curr. Microbiol.* **36**, 183–189.
11. Whitehead, T. R. and Cotta, M. A. (2001), *Curr. Microbiol.* **43**, 293–298.
12. Nurizzo, D., Turkenburg, J. P., Charnock, S. J., et al. (2002), *Nat. Struct. Biol.* **9**, 665–668.
13. Gill, S. C. and von Hippel, P. H. (1989), *Anal. Biochem.* **182**, 319–326.
14. Kezdy, F. J. and Bender, M. L. (1962), *Biochemistry* **1**, 1097–1106.
15. Guex, N. and Peitsch, M. C. (1997), *Electrophoresis* **18**, 2714–2723.
16. García de la Torre, J., Huertas, M. L., and Carrasco, B. (2000), *Biophys. J.* **78**, 719–730.